Macromolecules
Article
Cite This: *Macromolecules* 2019, 52, 4139−4144
pubs.acs.org/Macromolecules

Stability Limits of Pressure Densified Polycarbonate Glass

A. P. Holt,[†] D. Fragiadakis,[†] J. A. Wollmershauser,[#] B. N. Feigelson,[‡] M. Tyagi,[§,∥] and C. M. Roland*[,†]

[†]Chemistry Division, [#]Materials Science & Technology Division, and [‡]Electronic Science & Technology Division, Naval Research Laboratory, Washington, D.C. 20375, United States

[§]Center for Neutron Research, National Institute of Standards and Technology, Gaithersburg, Maryland 20899-6100, United States

[∥]Department of Materials Science and Engineering, University of Maryland, College Park, Maryland 20742, United States

ABSTRACT: The physical properties of a polycarbonate (PC) glass formed under high pressure are evaluated experimentally and compared to molecular dynamics simulations of a simple model polymer capable of pressure densification. Pressure densified glass (PDG) exhibits higher enthalpy and is as much as 4% denser than the corresponding glass formed at ambient pressure. Measurements of the first sharp diffraction peak reveal that local density fluctuations are suppressed in PDG, as corroborated by elastic incoherent neutron scattering measurements. Both the experimental and simulation results indicate that the reduced stability of PDG limits the pressures for which pressure densification is effective; at too high a pressure the glass transition temperature falls below ambient.

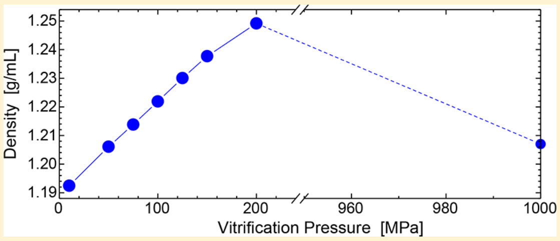

INTRODUCTION

Glasses are nonequilibrated materials, with their structure and properties dependent on the thermodynamic path used to vitrify the liquid. Understanding, manipulating, and exploiting the full potential of the nonequilibrium state of glasses is a challenge that offers the possibility of better properties and more stable materials. One approach is pressure densification,[1−9] which refers to the application of pressure to a liquid or polymer melt, followed by cooling to the vitreous state. The subsequent release of the pressure yields a pressure densified glass (PDG) at the same temperature and pressure (i.e., ambient) of the corresponding conventional glass (CG); however, the PDG has different properties, for example, higher density and modest changes in mechanical behavior.[5,10] Thus, pressure densification affords the ability to tune the structure of the glass by employing different temperature and pressure histories.

In this work, we characterize differences in the static and dynamic properties of polycarbonate glasses prepared by densification at various pressures, including very high pressure (1 GPa). Scattering measurements indicate changes in the static structure of the PDG, with a decrease in local density fluctuations. Thermodynamically, the PDG exhibits higher enthalpy and less thermal stability than CG, notwithstanding a mass density closer to the equilibrium value. This reduced stability limits the pressures that can be applied to attain PDG. To better understand these results, our experimental findings are augmented with molecular dynamics (MD) simulations of chain molecules.

EXPERIMENTAL SECTION

The material was polycarbonate (Makrolon GP from Covestro), used as received. Most pressured densified samples herein were prepared in a Gnomix apparatus,[11] having a pressure range of 10−200 MPa, with the sample confined by mercury. The specific volume was measured in situ, typically at temperatures from 25 to 300 °C. The rate of heating and cooling was 0.5 K/min. An additional pressure densification was performed at 1 GPa using a multianvil, split-sphere apparatus.[12,13] For this experiment the PC was heated to 320 °C, followed by slow increase of the pressure. At 1 GPa the temperature was increased to 370 °C and held constant for 5 min. Following cooling to ambient temperature, the pressure was reduced to atmospheric.

Mass densities were obtained at ambient conditions by pycnometry (Quantachrome UltraPyc 1200e) with helium as the confining fluid. The measurement was repeated several times, with an accuracy better than 0.02%.

Wide-angle X-ray scattering (WAXS) experiments employed a Rigaku SmartLab ($\lambda = 1.54$ Å) in the Bragg−Brentano geometry, with 2θ from 2° to 30°. Scattering from the borosilicate sample holders was measured separately and subtracted from the scattering profiles. All data were normalized by the integrated area to account for the sample mass.

Temperature-modulated differential scanning calorimetry using a TA Instruments Q100 was performed at a heating rate of 1 K/min, with modulation amplitude = 0.16° and period = 40 s.

Elastic incoherent neutron scattering (EINS) measurements were obtained using the high-flux backscattering (HFBS) instrument at NIST in the fixed window scan mode. In this mode all elastically scattered neutrons within the instrument resolution of 0.8 μeV are counted. Samples were held in annular aluminum holders, with a

Received: March 25, 2019
Revised: April 22, 2019
Published: May 31, 2019

DOI: 10.1021/acs.macromol.9b00603
Macromolecules 2019, 52, 4139−4144

thickness of 0.1 mm to avoid multiple scattering. Initially cooled to 15 K, at which the scattering is completely elastic, samples were heated at 0.4 K/min, sufficiently slow to avoid temperature gradients, with data collected every 75 s.

Molecular dynamics simulations (MDs) were performed in the NPT ensemble using the RUMD software[14] modified to incorporate a Berendsen barostat.[15] A total of 8000 Lennard-Jones particles were simulated (80 polymer chains ×100 segments). Nonbonded segments interact through a Lennard-Jones potential with the interparticle distance and the potential well depth both set to unity. All MDs results are given in dimensionless Lennard-Jones units. Bond lengths were kept approximately constant (within 1%) at 0.5 using harmonic bonds with a large force constant = 10^5. Bond angles were equal to 120°, maintained constant (within a few degrees) by means of a stiff harmonic bond angle potential, with spring constant = 1000. A simple sinusoidal torsional potential, $U(\theta) = 0.5A(1 + \cos 3\theta)$, where θ is the dihedral angle and $A = 10$, was used.

■ RESULTS AND DISCUSSION

Pressure Densification of Polycarbonate. The pressure densification experiments were performed by application of high pressure to the PC above T_g, followed by isobaric, slow cooling to the glass state (Figure 1). The greater density of the PDG is in accord with the general behavior of glass-forming materials, including polymers. It also confirms previous findings[1,2] that "simple" liquids deviate from the prediction of isomorph theory.[16,17] This is noteworthy since PC has a Prigogine−Defay ratio close to unity, which identifies it as a material expected to have properties strongly complying with the theory.[18]

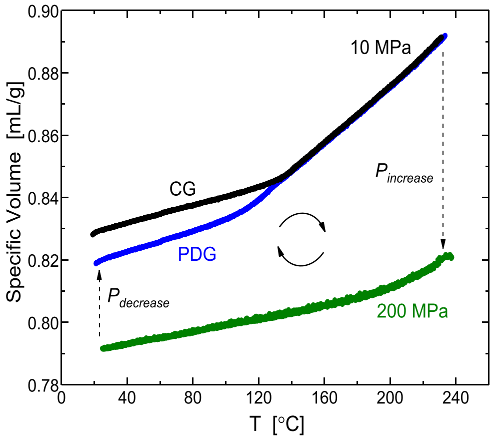

Figure 1. Isobaric specific volume for PC as a function of temperature for pressure densification performed by heating from the glassy state (uppermost curve); applying pressures up to 200 MPa, followed by cooling to room temperature (lowest curve); and releasing the pressure and heating through the glass transition (middle curve).

The measurements in the Gnomix apparatus are illustrated in Figure 2, with vitrification pressures as high as 200 MPa. Note that when the PDG is heated, a change in thermal expansivity occurs prior to reaching the glass transition temperature, T_g. Johari[9] has ascribed this sub-T_g feature to the instability of PDG due to their high density and high enthalpy.

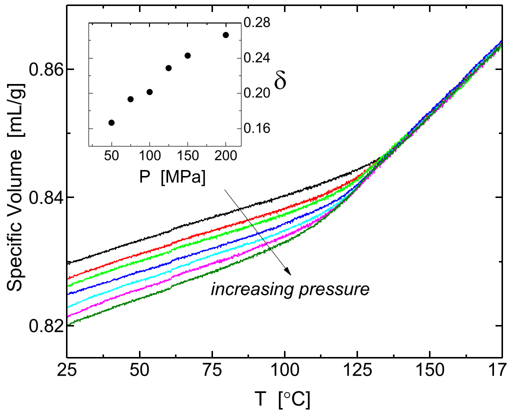

Figure 2. Temperature dependence of the specific volume on heating for polycarbonate vitrified at 10, 50, 75, 100, 125, 150, and 200 MPa. The extent of pressure densification (eq 3) is shown in the inset.

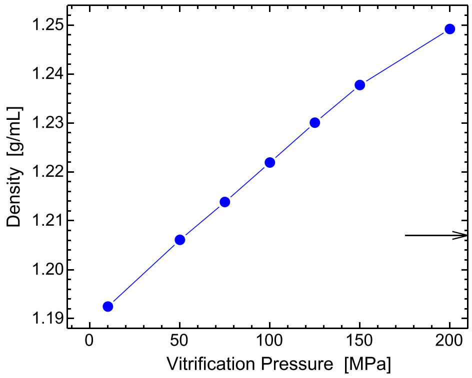

Figure 3. Mass density at ambient conditions for polycarbonate PDG formed at the indicated pressures. The arrow indicates the density of PC vitrified at 1 GPa.

As the vitrification pressure increases, there is more densification of the PC. Collected in Figure 3 are the densities for various vitrification pressures. At the highest pressure for the experiments in the Gnomix (= 200 MPa), the increase in density exceeds 4%. A measure of the extent of pressure densification is the compressibility at low pressure resulting from glass formation at a pressure, P_1[19]

$$\kappa' = \nu_{CG}{}^{-1}\frac{\nu_{CG} - \nu_{PDG}(P_0)}{P_1} \tag{2}$$

where ν_{CG} and $\nu_{PDG}(P_0)$ are the respective specific volumes of the conventional CG and the PDG, both measured at ambient pressure, P_0. As the vitrification pressure increases, κ' decreases. Our results are consistent with a value previously reported for PC, $\kappa' = 5.1 \times 10^{-2}$ GPa^{-1} for vitrification at $P_1 = 10$ MPa.[10] The compressibility for PC vitrified herein at 200 MPa was $\kappa' = 5.9 \times 10^{-2}$ GPa^{-1}.

A second metric of pressure densification is[17]

$$\delta = \frac{\nu_{CG} - \nu_{PDG}(P_0)}{\nu_{CG} - \nu_{PDG}(P_1)} \tag{3}$$

where $\nu_{PDG}(P_1)$ refers to the specific volume of the PDG prior to the release of the vitrifying pressure. This parameter is plotted versus vitrification pressure in the inset to Figure 2. For the highest pressure, 200 MPa, $\delta = 0.27$, which is within the range found generally for polymers, $0.14 < \delta < 0.30$.[1,17]

Because the extent of pressure densification increases with vitrification pressure through 200 MPa, an experiment was performed in which PC was heated in the multianvil, split-sphere device above T_g, with the pressure then raised to 1 GPa. The temperature required for the PC to be initially a melt at 1

GPa was estimated from determination of the effect of pressure on the T_g of conventional PC. These results are collected in Figure 4, along with literature data (the latter vertically shifted to coincide with the present measurements). Simultaneously fitting the two data sets to the equation of Andersson and Andersson[20]

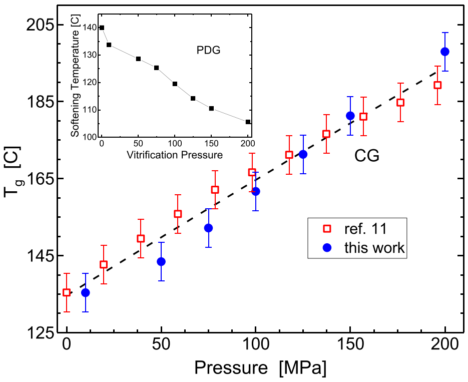

Figure 4. Pressure-dependent glass transition temperature of polycarbonate CG along with the fit of eq 4. Data herein measured during cooling in the Gnomix at the indicated pressure. Inset shows the glass transition temperature during heating from the expansivity data in Figure 2; extrapolation indicates a subambient T_g for PC glass formed at 1 GPa.

$$T_g(P) = T_g(0)\left(1 + \frac{a}{b}P\right)^{1/a} \tag{4}$$

we obtain $a = 1.4 \pm 2$ and $b = 1340 \pm 220$ MPa, with values of $T_g = 408 \pm 2$ K at ambient pressure and 680 K at 1 GPa. (Note eq 4 is analogous to the Simon−Glatzel equation for the pressure dependence of the melting point.[21])

The multiaxis anvil assembly does not allow for *in situ* density measurements. The density at ambient pressure and temperature measured after removal from the assembly is indicated in Figure 3 by the arrow. It is less than 0.7% larger than the CG and lower than any of the PDG prepared in the Gnomix at pressures beyond 75 MPa. From eq 2 we obtain $\kappa' = 6.8 \times 10^{-3}$ GPa^{-1} for the $P = 1$ GPa PDG, which is an order of magnitude smaller than achieved at lower pressures.

This counterintuitive result—higher pressure effects less pressure densification—is an artifact of the lower stability of PDG; that is, the glass formed a 1 GPa transitions to the amorphous liquid when the pressure is removed. The lower stability of the PDG is seen in Figure 2; the temperature at which the PC on heating assumes the thermal expansivity of the melt, an effective T_g, decreases with increasing vitrification pressure. In Figure 5 are calorimetry results showing the higher enthalpy of the PDG formed at 200 MPa in comparison to the CG. The lower stability of the PDG with increasing vitrification pressure is also seen in the inset to Figure 4. There is a monotonic decrease in T_g with densification pressure. Estimating T_g for the PDG formed at 1 GPa requires an overly long extrapolation; nevertheless, it is clear that on release of the pressure the structure of the PDG prepared at 1 GPa is lost. The material revitrifies at a lower pressure and indeterminate temperature. Thus, the reduced stability of PDG imposes an upper bound on the vitrification pressure. This limitation of pressure densification is not a fundamental problem but depends on the material and T_g of the PDG at the temperature and pressure of interest, typically ambient. The rest of the analysis herein was limited to PC vitrified at 200 MPa or less.

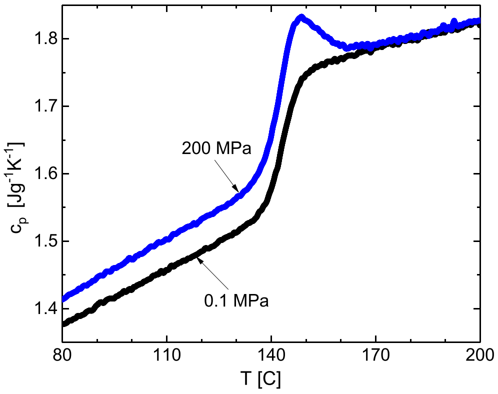

Figure 5. Heat capacity for polycarbonate vitrified at 0.1 MPa (lower curve) and 200 MPa (upper curve).

Consistent with its lower stability, the structure of PDG is not at equilibrium. Vitreous materials lack long-range order but typically show static correlations at intermediate length scales. This indicates a degree of structural regularity other than the local liquid structure giving rise to an amorphous halo in scattering measurements. Experimentally, this intermediate range order is manifested as the so-called first sharp diffraction peak (FSDP) in the static structure factor, $S(Q)$, measured by elastic X-ray or neutron scattering.

The FSDP at $Q \sim 1.2$ Å^{-1} are shown in Figure 6 for CG and PDG PC glasses. The primary difference is a reduced magnitude of the FSDP for the PDG (6 ± 3%), with the position of the peak not significantly affected. If the peak amplitude of the FSDP is determined primarily by the Debye−Waller factor,[22] the PDG exhibits reduced local density fluctuations. Although our results are consistent with previous work on pressure densified polystyrene[23] and lithium silicate,[24,25] it should be noted that there is a lack of consensus regarding the origin of the FSDP in amorphous glasses.[26,27] The main conclusion from Figure 6 is that pressure densification subtly alters the intermediate range order.

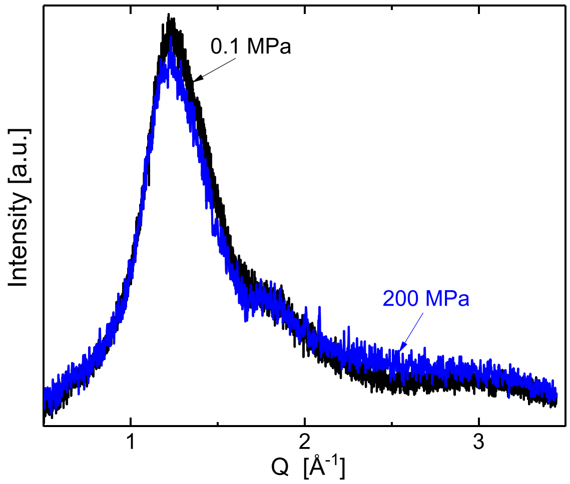

Figure 6. WAXS profiles showing the first sharp diffraction peak of polycarbonate CG (black) and PDG (blue).

To better understand the influence of vitrification pressure on the sub-T_g dynamics, EINS was carried out, with the elastic scattering intensity, $S_{inc}(Q, \omega = 0)$, measured as a function of temperature during heating of the glassy PC (samples same as those in Figure 6). The temperature-dependent mean-square-displacement (MSD), calculated using the Debye–Waller approximation,[28] is shown in Figure 7 for the CG and PDG.

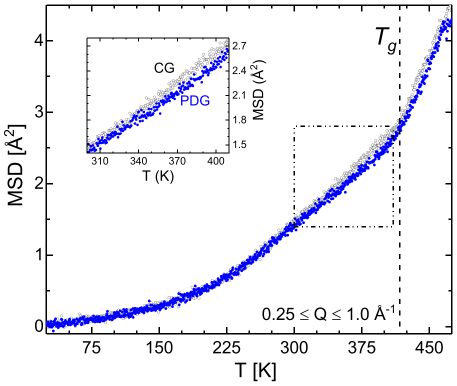

Figure 7. Average mean-square displacement (MSD) of CG (hollow) and PDG (solid) upon heating from the glassy state. Inset: close-up of the boxed region to more clearly show the reduced amplitude of the MSD for the PDG.

This MSD reflects density fluctuations occurring from 0.03 ps to 2 ns. The glasses exhibit no significant differences in the MSD well below T_g. This is unsurprising since molecular motions at temperatures below 150 K are primarily methyl group rotations, not expected to be sensitive to density changes. However, on approach to T_g (300 K < T < 400 K) the amplitude of the MSD is reduced for PDG. Similar results (not shown) were obtained for PC pressurized at lower pressures, with the reduction in the MSD increasing with increasing vitrification pressure. The data indicate a suppression of local density fluctuations, consistent with the FSDP in Figure 6. The exact motion underlying these fluctuations is difficult to discern due to the complex structure of the polycarbonate backbone.

Molecular Dynamics Simulations. We simulate the pressure densification process for a coarse-grained model polymer, similar to that used in ref 29. This model does not specifically represent polycarbonate but rather is the simplest polymer that shows pressure densification behavior similar to that seen experimentally. The most basic model polymer, a freely jointed chain, does not pressure densify, while a freely rotating chain pressure densifies to a much lesser extent than observed for any real polymer.[3] We were able to obtain realistic pressure densification behavior by incorporating a torsional potential $U_T(\theta) = 0.5A(1 + \cos 3\theta)$ where θ is the dihedral angle, with a torsional barrier height $A = 10$. We found that the exact form of the torsional potential (e.g., number and depths of minima) does not qualitatively affect the results; the degree of pressure densification increases with increasing torsional barrier height.

To create the simulated glass, a well-equilibrated melt was cooled isobarically at a rate of 10^{-4} (temperature/time units) to $T = 1$ at $P = 1$ (CG) or higher (PDG). The latter was decompressed to $P = 1$ over a time $t = 100$ after reaching $T = 0.1$. The volumes during formation of PDG and subsequent heating of CG and PDG are shown in Figure 8 for $P_1 = 10$. The expected change is observed in the slope of $V(T)$ at T_g. The volume data reflect significant pressure densification, $\kappa' = 1.1 \times 10^{-3}$ and $\delta = 0.36$. Similar to PC (Figure 1) there is an increase in apparent thermal expansivity of the PDG on heating prior to reaching T_g.

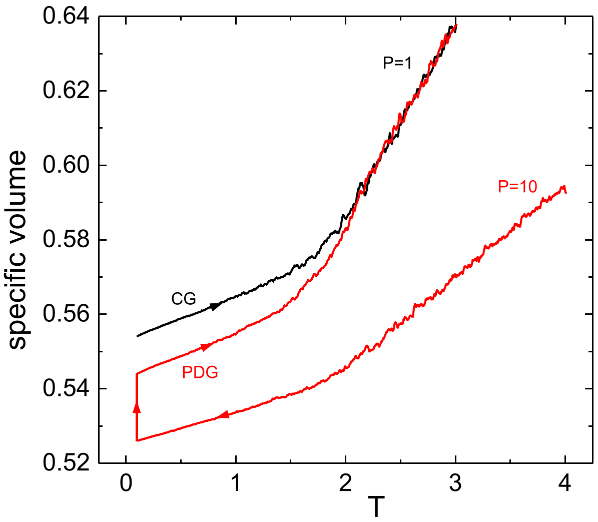

Figure 8. Temperature dependence of specific volume for simulated polymer cooled at $P = 10$ and depressurized to form PDG as well as subsequent heating of PDG. Heating of CG formed at $P = 1$ is also shown.

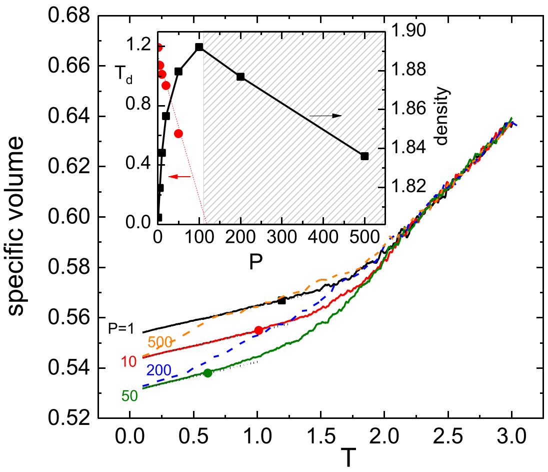

Figure 9. Temperature dependence of specific volume on heating for PDGs formed at various densification pressures. The inset shows the temperature T_d at which $V(T)$ deviates from its low-temperature behavior as well as the density of the glass at $T = 0.1$ as a function of densification pressure; the shaded area indicates the region where PDGs are unstable.

Figure 9 shows the temperature dependence of specific volume for simulated glasses formed at several densification pressures as well as the conventional glass. For densification pressures $P_1 < 100$ the PDG's density at the lowest temperature (shown in the inset) increases with densification pressure similar to what is seen in Figure 2 for polycarbonate. Above this pressure, the density *decreases* with increasing densification pressure. We also observe that for $P_1 < 100$ the low-temperature apparent thermal expansivity of the PDG is similar to that of the CG up to a temperature T_d, after which it begins to increase. T_d is a measure of stability: if held at $T > T_d$, the volume will increase slowly with time, approaching that of the CG. Note that this destabilization temperature T_d (shown in the inset to Figure 9) decreases rapidly with densification pressure, reaching near zero around $P_1 = 100$, the same pressure as the density maximum. This suggests that the maximum in density arises from the fact that pressure densified glasses formed at $P_1 > 100$ are unstable even at the lowest temperatures and relax to lower density immediately after pressure is released, which corroborates the conclusions reached above for polycarbonate.

In Figure 10 we compare the mean-square displacement (averaged for times between 1 and 10^3) for the CG and PDG.

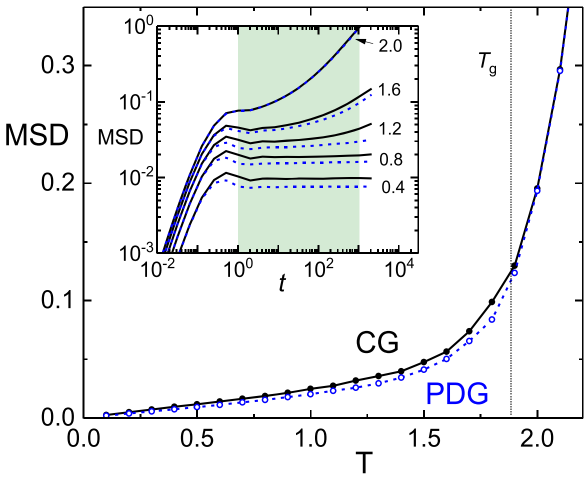

Figure 10. Mean-square displacement (MSD) of CG (black solid lines) and PDG (blue dashed lines) upon heating from the glassy state. Inset: MSD as a function of time for selected temperatures. MSD in the main plot is averaged between $t = 1$ and $t = 10^3$ (green shading in the inset).

Similar to polycarbonate, the pressure densified glass has lower MSD below the glass transition, the difference becoming most evident close to T_g. The change of slope at low temperature observed for polycarbonate is absent for the simulated polymer and probably arises from the onset of local motions in PC, lacking in the simulated polymer. The inset shows the MSD as a function of time; at very short times (ballistic regime) the MSD varies as t^2, with a plateau developing (caging regime), followed by an increase at longer times at temperatures close to and above the glass transition. On the logarithmic scale of the inset, it is clear that below the glass transition the mean-square displacement of the PDG is less than that of the CG by a factor that is essentially independent of time and temperature.

CONCLUSIONS

The physical properties of polycarbonate glasses and simulated model polymer glasses prepared through two different thermodynamic pathways, cooling at low or high pressure, were compared. Pressure densification yields a denser, less stable glass, the latter reflected in a higher enthalpy and lower glass transition temperature. There is also a suppression of density fluctuations in the PDG. Prior to reaching T_g during heating, there is an increase in thermal expansivity for the PDG. Evidently, the excess disorder arising during formation of the glass evolves toward the lower energy configuration of CG. This excess disorder lowers the stability and limits the magnitude of the pressure that can be utilized to form PDG.

AUTHOR INFORMATION

Corresponding Author

*E-mail: roland@nrl.navy.mil (C.M.R.).

ORCID

A. P. Holt: 0000-0003-2916-6963
D. Fragiadakis: 0000-0002-0259-3677
J. A. Wollmershauser: 0000-0002-4257-5406
C. M. Roland: 0000-0001-7619-9202

Notes

The authors declare no competing financial interest.

ACKNOWLEDGMENTS

This work was supported by the Office of Naval Research, in part by ONR Code 332 (R. Barsoum). A.P.H. acknowledges an ASEE postdoctoral fellowship. Access to the HFBS was provided by the Center for High Resolution Neutron Scattering, a partnership between NIST and the National Science Foundation under Agreement No. DMR-1508249. Certain commercial instruments or materials are identified in this paper in order to specify the experimental procedure adequately, but do not imply recommendation or endorsement by NIST.

REFERENCES

(1) Casalini, R.; Roland, C. M. Effect of density on the physical aging of pressure-densified polymethylmethacrylate. *J. Chem. Phys.* **2017**, *147*, No. 091104.

(2) Casalini, R.; Roland, C. M. Pressure densification of a simple liquid. *J. Non-Cryst. Solids* **2017**, *475*, 25−27.

(3) Fragiadakis, D.; Roland, C. M. A test for the existence of isomorphs in glass-forming materials. *J. Chem. Phys.* **2017**, *147*, No. 084508.

(4) Andersson, O.; Johari, G. P. Sub-T_g features of glasses formed by cooling glycerol under pressure − Additional incompatibility of vibrational with configurational states in the depressurized, high density glass. *J. Chem. Phys.* **2016**, *145*, 204506.

(5) Hutchinson, J. M. In *The Physics of Glassy Polymers*; Haward, R. N., Ed.; Springer: 1997; Chapter 3.

(6) Casalini, R.; Roland, C. M. Anomalous properties of the local dynamics in polymer glasses. *J. Chem. Phys.* **2009**, *131*, 114501.

(7) Danilov, I. V.; Gromnitskaya, E. L.; Brazhkin, V. V. Vivid Manifestation of Nonergodicity in Glassy Propylene Carbonate at High Pressures. *J. Phys. Chem. B* **2016**, *120*, 7593−7597.

(8) Ding, J.; Asta, M.; Ritchie, R. O. Anomalous structure-property relationships in metallic glasses through pressure-mediated glass formation. *Phys. Rev. B: Condens. Matter Mater. Phys.* **2016**, *93*, 140204.

(9) Johari, G. P. Comment on 'Water's second glass transition and the sub-T_g features of pressure-densified glasses'. *Thermochim. Acta* **2015**, *617*, 208−218.

(10) Bree, H. W.; Heijboer, J.; Struik, L. C. E.; Tak, A. G. M. The effect of densification on the mechanical properties of amorphous glassy polymers. *J. Polym. Sci., Polym. Phys. Ed.* **1974**, *12*, 1857−1864.

(11) Zoller, P.; Walsh, D. J. *Standard Pressure-Volume-Temperature Data for Polymers*; Technomic: Lancaster, PA, 1995.

(12) Vins, V. G.; Feigelson, B. N.; Eliseev, A. P.; Patrin, N. S.; Patrenin, Y. V.; Nehaev, P. Y. Optically Active Defects in Diamonds Grown at 1350−1740°C. *J. Superhard Mater./Sverkhtverdye Mater.* **1991**, *3*, 21−26.

(13) Wollmershauser, J. A.; Feigelson, B. N.; Qadri, S. B.; Villalobos, G. R.; Hunt, M.; Imam, M. A.; Sanghera, J. S. Transparent Nanocrystalline Spinel by Room Temperature High-pressure Compaction. *Scr. Mater.* **2013**, *69*, 334−337.

(14) Bailey, N.; Ingebrigtsen, T.; Hansen, J. S.; Veldhorst, A.; Bøhling, L.; Lemarchand, C.; Olsen, A.; Bacher, A.; Costigliola, L.;

Pedersen, U.; Larsen, H.; Dyre, J.; Schroder, T. RUMD: A general purpose molecular dynamics package optimized to utilize GPU hardware down to a few thousand particles. *SciPost Phys.* **2017**, *3*, No. 038.

(15) Berendsen, H. J.; Postma, J. V.; van Gunsteren, W. F.; DiNola, A. R. H. J.; Haak, J. R. Molecular dynamics with coupling to an external bath. *J. Chem. Phys.* **1984**, *81*, 3684−3690.

(16) Gnan, N.; Maggi, C.; Schrøder, T. B.; Dyre, J. C. Predicting the effective temperature of a glass. *Phys. Rev. Lett.* **2010**, *104*, 125902.

(17) Fragiadakis, D.; Roland, C. M. A test for the existence of isomorphs in glass-forming materials. *J. Chem. Phys.* **2017**, *147*, No. 084508.

(18) Gundermann, D.; Pedersen, U. R.; Hecksher, T.; Bailey, N. P.; Jakobsen, B.; Christensen, T.; Olsen, N. B.; Schrøder, T. B.; Fragiadakis, D.; Casalini, R.; Roland, C. M.; Dyre, J. C.; Niss, K. Predicting the density-scaling exponent of a glass-forming liquid from Prigogine-Defay ratio measurements. *Nat. Phys.* **2011**, *7*, 816−821.

(19) McKinney, J. E.; Simha, R. Thermodynamics of the densification process for polymer glasses. *J. Res. Natl. Bur. Stand., Sect. A* **1977**, *81*, 283−297.

(20) Andersson, S. P.; Andersson, O. Relaxation studies of poly(propylene glycol) under high pressure. *Macromolecules* **1998**, *31*, 2999−3006.

(21) Rzoska, S. J. New challenges for the pressure evolution of the glass temperature. *Front. Mater.* **2017**, *4*, 33.

(22) Voylov, D. N.; Griffin, P. J.; Mercado, B.; Keum, J. K.; Nakanishi, M.; Novikov, V. N.; Sokolov, A. P. Correlation between temperature variations of static and dynamic properties in glass-forming liquids. *Phys. Rev. E: Stat. Phys., Plasmas, Fluids, Relat. Interdiscip. Top.* **2016**, *94*, No. 060603.

(23) Curro, J. J.; Roe, R. J. Small-angle x-ray scattering study of density fluctuation in pressure-densified polystyrene glasses. *J. Polym. Sci., Polym. Phys. Ed.* **1983**, *21* (9), 1785−1796.

(24) Kitamura, N.; Fukumi, K.; Mizoguchi, H.; Makihara, M.; Higuchi, A.; Ohno, N.; Fukunaga, T. High pressure densification of lithium silicate glasses. *J. Non-Cryst. Solids* **2000**, *274*, 244−248.

(25) Buchner, S.; Pereira, A. S.; Cardoso de Lima, J.; Balzaretti, N. M. X-ray study of lithium disilicate glass: High pressure densification and polyamorphism. *J. Non-Cryst. Solids* **2014**, *387*, 112−116.

(26) Elliott, S. R. Origin of the first sharp diffraction peak in the structure factor of covalent glasses. *Phys. Rev. Lett.* **1991**, *67*, 711.

(27) Crupi, C.; Carini, G.; González, M.; D'Angelo, G. Origin of the first sharp diffraction peak in glasses. *Phys. Rev. B: Condens. Matter Mater. Phys.* **2015**, *92*, 134206.

(28) Soles, C. L.; Douglas, J. F.; Wu, W. L.; Dimeo, R. M. Incoherent neutron scattering as a probe of the dynamics in molecularly thin polymer films. *Macromolecules* **2003**, *36*, 373−379.

(29) Ransom, T. C.; Fragiadakis, D.; Roland, C. M. The α and Johari-Goldstein relaxations in 1,4-polybutadiene: Breakdown of isochronal superpositioning. *Macromolecules* **2018**, *51*, 4694−4698.

DOI: 10.1021/acs.macromol.9b00603
Macromolecules 2019, 52, 4139−4144